

## Static compression of iron-silicon alloys: Implications for silicon in the Earth's core

Jung-Fu Lin, Andrew J. Campbell, and Dion L. Heinz<sup>1</sup>

Department of the Geophysical Sciences, University of Chicago, Chicago, Illinois, USA

Guoyin Shen

Consortium for Advanced Radiation Sources, University of Chicago, Chicago, Illinois, USA

Received 17 May 2002; revised 11 October 2002; accepted 25 October 2002; published 28 January 2003.

[1] Three iron-silicon alloys ( $\text{Fe}_{85}\text{Si}_{15}$ ,  $\text{Fe}_{71}\text{Si}_{29}$ , and  $\epsilon\text{-FeSi}$ ) have been studied in a diamond anvil cell at room temperature up to 55 GPa by in situ energy-dispersive X-ray diffraction techniques. A body centered cubic (bcc) to hexagonal close packed (hcp) phase transformation in  $\text{Fe}_{85}\text{Si}_{15}$  began at 16 GPa and was completed by 36 GPa. No phase transformations were observed in either  $\text{Fe}_{71}\text{Si}_{29}$  or  $\epsilon\text{-FeSi}$  at high pressures, even when laser-heated to about 2000 K. The isothermal bulk modulus ( $K_{0T}$ ) of hcp- $\text{Fe}_{85}\text{Si}_{15}$  is 141 ( $\pm 10$ ) GPa with  $K'_{0T} = 5.70(\pm 0.60)$  and  $V_{02} = 6.882(\pm 0.031)$   $\text{cm}^3/\text{mol}$  (per molar atom). The  $K_{0T}$  of  $\text{Fe}_{71}\text{Si}_{29}$  is 199.0 ( $\pm 5.3$ ) GPa with  $K'_{0T} = 5.66(\pm 0.61)$  and  $V_0 = 6.887(\pm 0.014)$   $\text{cm}^3/\text{mol}$ , and the  $K_{0T}$  of  $\epsilon\text{-FeSi}$  is 184.7 ( $\pm 3.9$ ) GPa with  $K'_{0T}$  of 4.75 ( $\pm 0.37$ ) and  $V_0 = 6.790(\pm 0.007)$   $\text{cm}^3/\text{mol}$ . Our study indicates that the substitution of Si into iron would lower the density of iron, but significantly changes its compressibility neither in the bcc phase, nor at high pressures in the hcp phase. Upon comparison with the Preliminary Reference Earth Model, the calculated equations of state (EOS) of hcp- $\text{Fe}_{85}\text{Si}_{15}$ , using the Mie-Grüneisen EOS, indicate that an outer core containing about 8–10 wt.% Si and inner core containing about 4 wt.% Si in iron would satisfy the seismological constraints. Addition of silicon into iron increases the bulk sound velocity of iron, consistent with silicon being a light element in the Earth's core. **INDEX TERMS:** 1015 Geochemistry: Composition of the core; 3919 Mineral Physics: Equations of state; 3924 Mineral Physics: High-pressure behavior; 3954 Mineral Physics: X ray, neutron, and electron spectroscopy and diffraction; **KEYWORDS:** high pressure, light elements, iron-silicon alloy, Earth's core, X-ray diffraction, equation of state

**Citation:** Lin, J.-F., A. J. Campbell, D. L. Heinz, and G. Shen, Static compression of iron-silicon alloys: Implications for silicon in the Earth's core, *J. Geophys. Res.*, 108(B1), 2045, doi:10.1029/2002JB001978, 2003.

### 1. Introduction

[2] Geophysical and cosmochemical evidence indicates that iron is the most abundant component in the Earth's core. The simplest interpretation of the core is an inner core composed of a crystalline iron-nickel alloy and an outer core of liquid iron-nickel alloyed with a small fraction of lighter element(s) [Birch, 1952]. The density of the outer core is about 10% lower than the density of iron at core pressures and temperatures, while the bulk sound velocity of the core is about 3% higher than that of liquid iron [Birch, 1952; Dziewonski and Anderson, 1981; Ahrens, 1982; Anderson and Ahrens, 1994]. The difference in density between the core and the high-pressure phase of iron indicates the presence of a low-atomic-weight component in the outer core [Birch, 1952]. There

is also evidence that the inner core is less dense than pure iron, and the amount of light element in the inner core may be as much as several weight percent [Jephcoat and Olson, 1987; Anderson and Ahrens, 1994; Stixrude et al., 1997; Fiquet et al., 2001; Mao et al., 2001]. A number of light elements (H, C, N, O, Mg, Si, S) have been considered by various workers [e.g., Poirier, 1994; Hillgren et al., 2000].

[3] Silicon has been proposed to be an important alloying element in the Earth's core, based on its cosmochemical abundance [Ringwood, 1966] and the thermoelastic properties of iron-silicon alloys in shock-wave experiments [Balchan and Cowan, 1966; Matassov, 1977]. Allègre et al. [1995] used the ratios of major and trace elements in the mantle and in meteorite groups to estimate the possible silicon content in the core, and concluded that the core may contain about 7.3 wt.% Si in addition to other light elements. Silicon solubility in liquid iron-rich metal increases with decreasing oxygen fugacity, increasing pressure, and increasing temperature, and a few weight percent of silicon may dissolve into liquid iron at the base of a deep magma ocean ( $\sim 700$  km depth,  $\sim 25$  GPa) [Gessmann et al., 2001].

<sup>1</sup>Also at James Franck Institute, University of Chicago, Chicago, Illinois, USA.

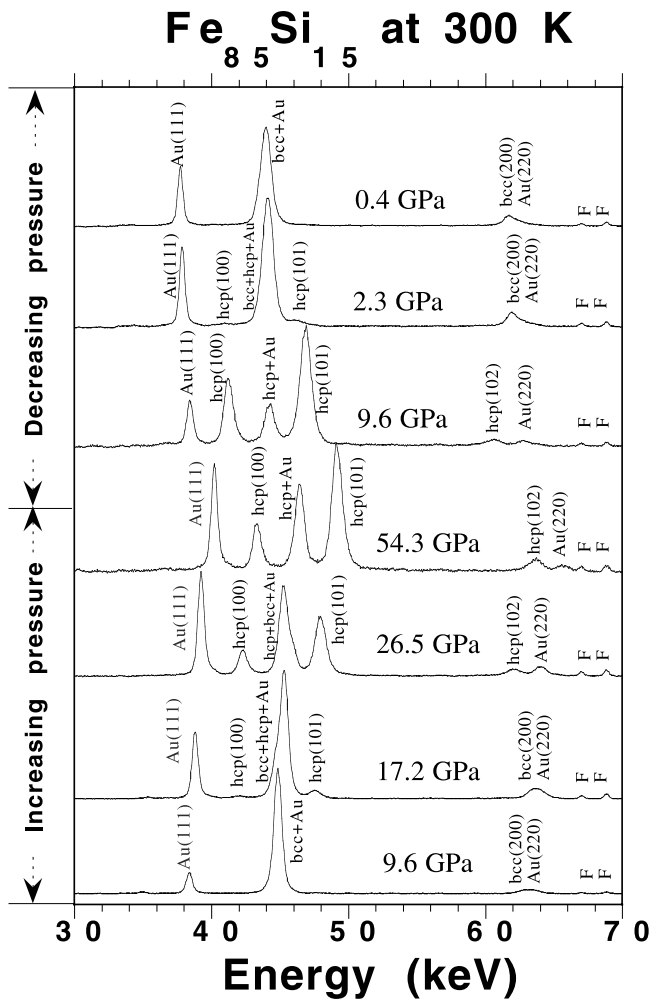


**Figure 1.** A series of X-ray diffraction patterns of  $\text{Fe}_{85}\text{Si}_{15}$  at increasing pressures to 54.3 GPa and then at decreasing pressures at 300 K. Diffraction peaks from the bcc and hcp phases of the alloy are indicated. F, the fluorescence peaks of gold; Au, the internal pressure calibrant.

To generate a core containing  $\sim 7.3$  wt.% Si as estimated by *Allègre et al.* [1995], a low oxygen fugacity during accretion [Ringwood, 1966] or possibly a magma ocean extending to 850 km ( $\sim 30$  GPa) [Gessmann et al., 2001] would be required. Studies of chemical reactions between mantle silicates and molten iron have also indicated that Fe-Si alloys may form at the core-mantle boundary ( $D''$  zone) [Knittle and Jeanloz, 1989, 1991]. Shock experiments on Fe-Si alloys suggested that an outer core containing 14–20 wt.% Si in iron is sufficient to satisfy the density deficit of the core [Balchan and Cowan, 1966; Matassov, 1977].

[4] Nevertheless, silicon was excluded as the primary alloying element in the outer core based on the relatively high bulk modulus ( $K_0$ ) and low-pressure derivative of the bulk modulus ( $K'_0$ ) of an intermediate compound, iron silicide ( $\epsilon$ -FeSi) [Knittle and Williams, 1995]. Since the sound velocity of liquid iron is essentially parallel to the Preliminary Reference Earth Model (PREM) velocity profile [Anderson and Ahrens, 1994], a lower value of  $K'_0$  of iron-silicon alloy would not be able to compensate for the

effect of significant Si within the outer core [Williams and Knittle, 1997]. In contrast, a recent static study on the equation of state (EOS) of a body-centered cubic (bcc)- $\text{Fe}_{84}\text{Si}_{16}$  (in atomic percent) alloy up to 9 GPa and 773 K concluded that substitution of silicon in iron would not significantly change the compressibility of the iron-rich Fe-Si alloy [Zhang and Guyot, 1999].

[5] Therefore we studied the EOS of three Fe-Si alloys ( $\text{Fe}_{85}\text{Si}_{15}$ ,  $\text{Fe}_{71}\text{Si}_{29}$ , and  $\epsilon$ -FeSi) in a diamond anvil cell (DAC) to understand the elastic properties of various Fe-Si alloys under high pressures and to resolve the discrepancy between previous studies. We especially focused on the thermal EOS of iron-rich Fe-Si alloys because silicon alloyed with iron has a large effect upon the phase diagram of iron, and the iron-rich portion of the Fe-Si system is more applicable than  $\epsilon$ -FeSi to understanding the possible effect of Si on iron under core conditions [Lin et al., 2002]. The thermal EOS and bulk sound

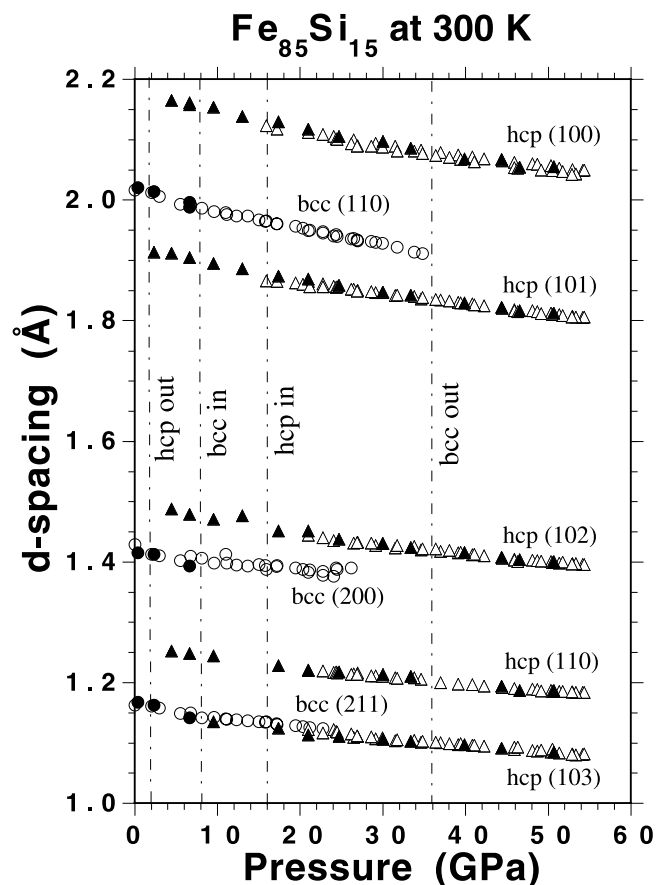


**Figure 2.** A plot of  $d$ -spacing versus pressure for  $\text{Fe}_{85}\text{Si}_{15}$  alloy under high pressures at 300 K. When the pressure was elevated above 16 GPa, a transformation to a hcp phase was clearly observed (indicated as hcp in). This phase transition was completed by 36 GPa (indicated as bcc out). The first appearance of the bcc phase during the quench process occurred at about 8 GPa (bcc in), and the hcp phase can still be seen above 2 GPa (hcp out). Open circles, bcc phase in increasing pressure; solid circles, bcc phase in decreasing pressure; open triangles, hcp phase in increasing pressure; solid triangles, hcp phase in decreasing pressure.

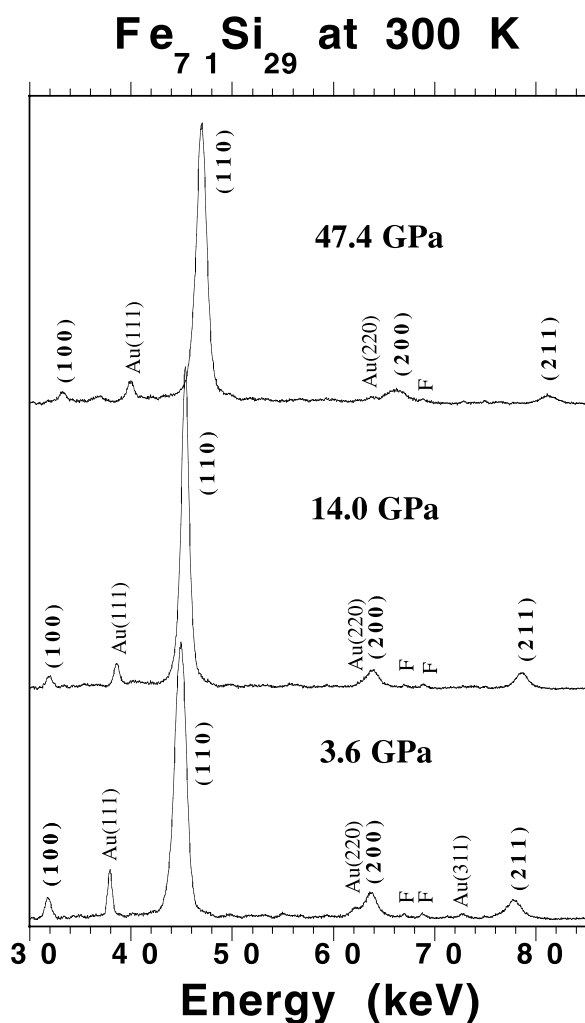


**Figure 3.** A series of X-ray diffraction patterns of  $\text{Fe}_{71}\text{Si}_{29}$  at increasing pressures to 47.4 GPa at 300 K. Diffraction peaks from the  $\text{Fe}_{71}\text{Si}_{29}$  phase are labeled in boldface. F, the fluorescence peaks of gold; Au, the internal pressure calibrant.

velocity of hexagonal close packed (hcp)- $\text{Fe}_{85}\text{Si}_{15}$  are calculated under core conditions, using our experimental data and the shock-wave data. The  $\text{Fe}_{71}\text{Si}_{29}$  and  $\epsilon$ -FeSi alloys were also laser heated in a DAC to understand the stability of the phases under high pressures and high temperatures.

## 2. Experiments

[6] The starting materials,  $\text{Fe}_{85}\text{Si}_{15}$  alloy (lot FE166010/6) and  $\text{Fe}_{71}\text{Si}_{29}$  alloy (lot FE176010/5), were purchased from Goodfellow Corporation and  $\epsilon$ -FeSi (iron silicide; lot C18G21) was obtained from Johnson Matthey. Electron microprobe analyses showed that the starting materials contained 7.9 ( $\pm 0.3$ ) wt.% Si, 17.0 ( $\pm 0.2$ ) wt.% Si, and 33.5 ( $\pm 0.3$ ) wt.% Si (each averaged from at least five analyses), respectively. Angle-dispersive X-ray diffraction at ambient conditions showed that the  $\text{Fe}_{85}\text{Si}_{15}$  was in bcc structure with  $a = 2.8520(\pm 0.0015)$  Å,  $\text{Fe}_{71}\text{Si}_{29}$  was in the

ordered B2 structure (space group:  $Pm\bar{3}m$ ) with  $a = 2.8108(\pm 0.0020)$  Å, and  $\epsilon$ -FeSi was in the B20 structure (space group:  $P2_13$ ) with  $a = 4.4846(\pm 0.0015)$  Å [Pauling and Soldate, 1948; Khalaff and Schubert, 1974; Kusbaschewski, 1982]. The B20 structure can be viewed as a distortion of the NaCl structure along [111] directions [Pauling and Soldate, 1948].

[7] Stainless steel gaskets were preindented to a thickness of 30  $\mu\text{m}$  and then drilled with a 100- $\mu\text{m}$  hole. The sample was ground into a fine powder with an average grain size of 2  $\mu\text{m}$  with gold powder added as the pressure standard [Heinz and Jeanloz, 1984a], and loaded into a DAC with ethanol-methanol (1:4) as the pressure medium. The ethanol-methanol pressure medium remains hydrostatic to almost 10 GPa [Piermarini *et al.*, 1973]; at high pressures it becomes a quasi-hydrostatic solid [Piermarini *et al.*, 1975]. Energy-dispersive synchrotron X-ray diffraction in a DAC was performed at Beamlines 13IDD and 13BMD, GSECARS sector of the Advanced Photon Source (APS), Argonne National Laboratory (ANL). The X-ray beam was focused to less than a 10- $\mu\text{m}$  spot onto the sample to minimize peak broadening caused by pressure gradients in

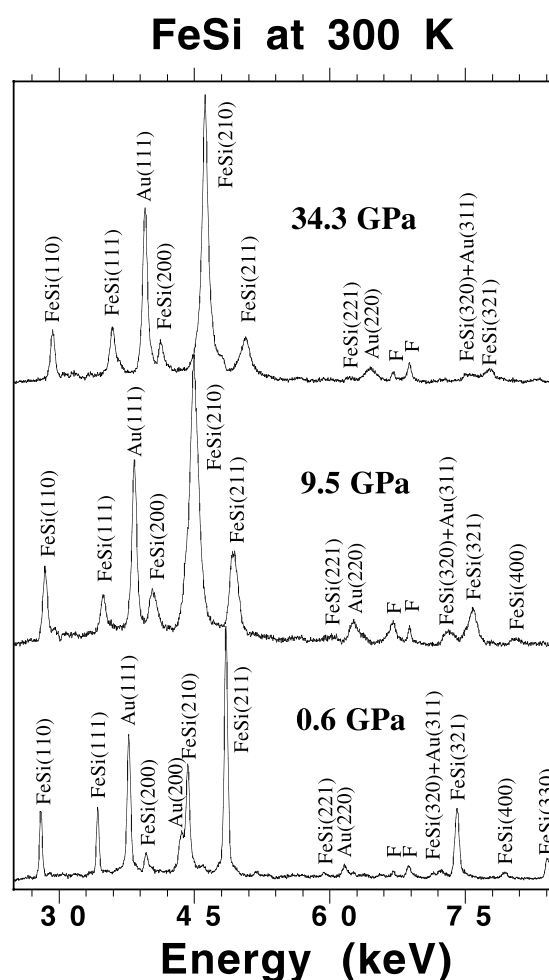


**Figure 4.** A series of X-ray diffraction patterns of  $\epsilon$ -FeSi at increasing pressures to 34.3 GPa at 300 K. F, the fluorescence peaks of gold; Au, the internal pressure calibrant.

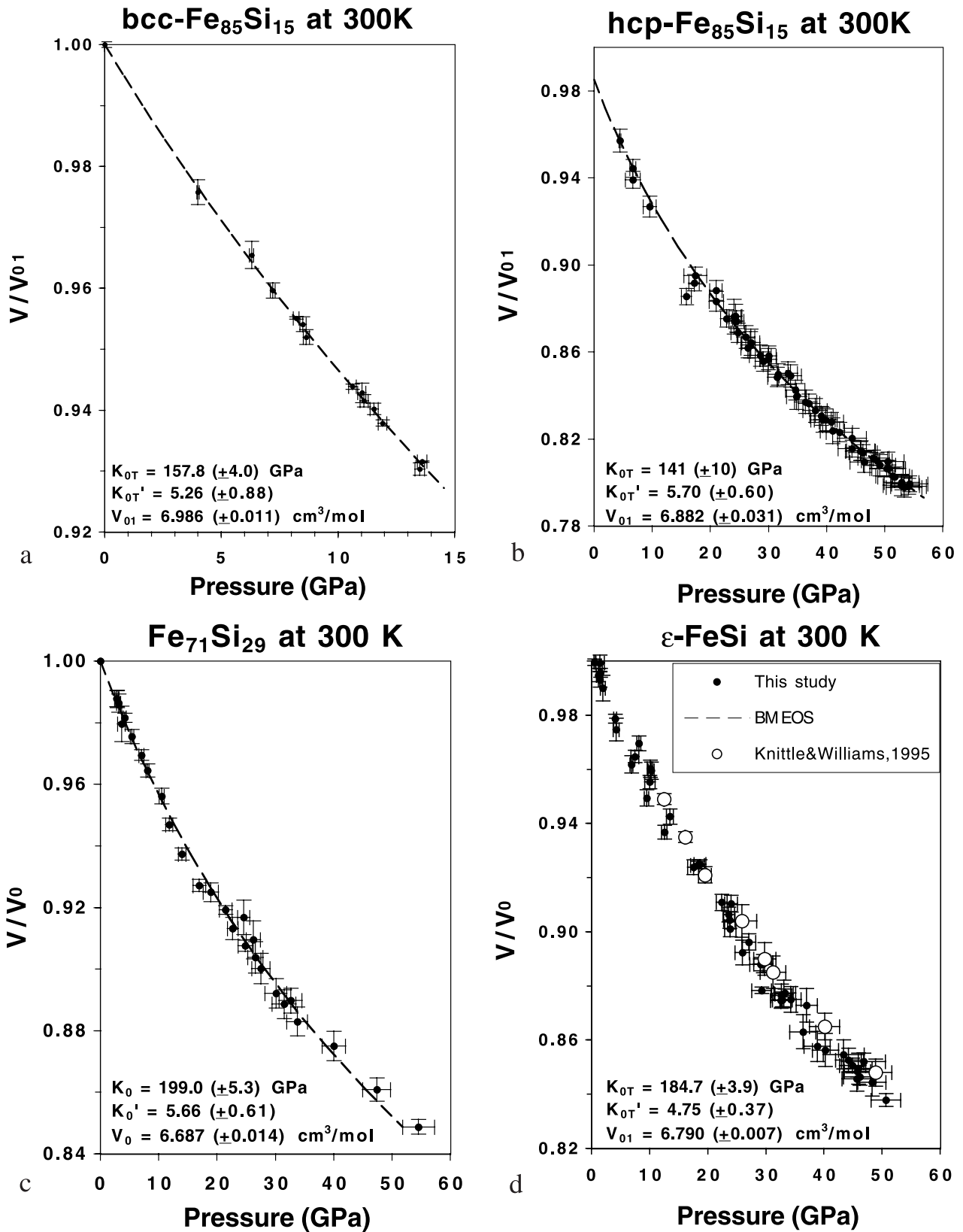


**Figure 5.** (a) Relative volume of bcc-Fe<sub>85</sub>Si<sub>15</sub> as a function of pressure at 300 K. Dashed line represents a weighted least squares fit. (b) Relative volume of the hcp-Fe<sub>85</sub>Si<sub>15</sub> as a function of pressure at 300 K. (c) Relative volume of the Fe<sub>71</sub>Si<sub>29</sub> as a function of pressure at 300 K. (d) Relative volume of the ε-FeSi as a function of pressure at 300 K (solid circles). Compression data for ε-FeSi collected by *Knittle and Williams* [1995] are also plotted for comparison (open circles). A lower  $V_0$  used by *Knittle and Williams* [1995] may cause the systematic discrepancy between the compression data.

the sample chamber. Two clean-up slits, 30  $\mu\text{m}$  in width, were used to cut off the tails of the focused X-ray beam. The energy calibration of the detector was accomplished using known energies of X-ray emission lines of several elements (Ag, Cd, and Co). The diffracted X rays were collected by a Ge solid state detector at a fixed  $2\theta$  angle of about  $8^\circ$  or  $12^\circ$ . The exposure times ranged from 5 to 10 min. The  $d$ -spacings of the sample and the internal standard were determined by fitting a Gaussian curve to each diffraction peak. Pressures were calculated from three to five diffraction lines from the set of (111), (200), (220), (311), and (222) for the gold standard [Heinz and Jeanloz, 1984a]. Three to five diffraction peaks from the set of (100), (101), (102), (110), and (103) were used to calculate the unit cell parameters of hcp-Fe<sub>85</sub>Si<sub>15</sub>. Three to four diffraction peaks from the set of (100), (110), (200), and (211) were used to calculate the unit cell volume of Fe<sub>71</sub>Si<sub>29</sub>. Three to six diffraction lines from the set of (110), (111), (210), (211), (221), and (321) were used to calculate the unit cell parameters of  $\epsilon$ -FeSi. Since all Fe-Si samples were in simple structures, the cell parameters of the samples were calculated from the  $d$ -spacings. Standard deviations of the cell parameters were calculated from the variation of the  $d$ -spacings.

[8] Since some of the X-ray diffraction peaks of Au overlapped with those of bcc-Fe<sub>85</sub>Si<sub>15</sub>, NaCl was mixed with the sample for use as a pressure calibrant in an externally heated DAC up to 14 GPa to measure the EOS of the bcc-Fe<sub>85</sub>Si<sub>15</sub> in a better way [Birch, 1978; Bassett *et al.*, 1993]. The diffracted X rays were collected at 300 K after the sample was annealed at about 800 K at high pressures to reduce the effects of nonhydrostaticity. Three diffraction peaks, (110), (200), and (211), were used to calculate the unit cell parameters for bcc-Fe<sub>85</sub>Si<sub>15</sub>.

[9] The Fe<sub>71</sub>Si<sub>29</sub> alloy (in ordered B2 structure) and the  $\epsilon$ -FeSi alloy (in B20 structure) were laser heated in a DAC using the methods of Lin *et al.* [2002] to investigate the stability of these phases under high pressures and high temperatures. A sandwiched sample configuration, using NaCl as both the thermal insulator and pressure calibrant, was used in this study [Birch, 1978; Heinz and Jeanloz, 1984b].

### 3. Results

[10] Fe<sub>85</sub>Si<sub>15</sub>, Fe<sub>71</sub>Si<sub>29</sub>, and  $\epsilon$ -FeSi were compressed up to 54.3, 54.5, and 50.7 GPa, respectively (Figures 1–4). A phase transformation in the Fe<sub>85</sub>Si<sub>15</sub> alloy from bcc to hcp was observed to begin near 16 GPa and was completed by 36 GPa (Figures 1 and 2). The first appearance of the bcc phase during quench occurred at about 8 GPa, and the hcp phase can still be seen above 2 GPa (Figure 2). The two-phase (bcc + hcp) zone in Fe<sub>85</sub>Si<sub>15</sub> extends over a wide pressure range of 20 GPa at 300 K, compared with 11 GPa for the same structural transition in iron [Huang *et al.*, 1987]. The volume change ( $\Delta V/V_0$ ) across the bcc-hcp phase transition is about  $-1.9\%$  or  $-0.13 \text{ cm}^3/\text{mol}$ .

[11] The pressure and volume data were analyzed with the Birch-Murnaghan equation of state (BM EOS) using a weighted least squares linear fit of the strain ( $f$ ) and the normalized stress ( $F$ ) to obtain values for  $K_{0T}$  and  $K'_{0T}$

**Table 1.** Static Compression Data for bcc-Fe<sub>85</sub>Si<sub>15</sub><sup>a</sup>

Run	$P$ , GPa	$\sigma$ ( $P$ ), GPa	$a$ , $\text{\AA}$	$\sigma$ ( $a$ ), $\text{\AA}$	$V/V_0$	$\sigma$ ( $V/V_0$ )
Fe8Sieh445	4.00	0.06	2.8288	0.0020	0.9758	0.0021
Fe8Sieh437	6.30	0.09	2.8188	0.0022	0.9655	0.0023
Fe8Sieh310	7.20	0.11	2.8131	0.0012	0.9596	0.0012
Fe8Sieh311	8.20	0.12	2.8087	0.0002	0.9551	0.0002
Fe8Sieh303	8.50	0.13	2.8077	0.0012	0.9541	0.0012
Fe8Sieh429	8.64	0.13	2.8056	0.0012	0.9520	0.0012
Fe8Sieh428	10.62	0.16	2.7976	0.0004	0.9439	0.0004
Fe8Sieh420	11.02	0.17	2.7966	0.0016	0.9428	0.0016
Fe8Sieh401	11.12	0.17	2.7953	0.0010	0.9415	0.0010
Fe8Sieh412	11.55	0.17	2.7940	0.0009	0.9402	0.0009
Fe8Sieh301	11.91	0.18	2.7917	0.0005	0.9379	0.0005
Fe8Sieh406	13.50	0.20	2.7842	0.0010	0.9304	0.0010
Fe8Sieh407	13.60	0.20	2.7854	0.0001	0.9316	0.0001

<sup>a</sup> $a_0 = 2.8520(\pm 0.0015) \text{ \AA}$  and  $V_0 = 6.985(\pm 0.011) \text{ cm}^3/\text{mol}$  at ambient conditions. The EOS of NaCl in B1 structure was used to determine the pressure [Birch, 1978].

[Birch, 1978; Jeanloz, 1981] (Figure 5 and Tables 1–4). The isothermal EOS parameters are given in Table 5.

[12] The Fe<sub>71</sub>Si<sub>29</sub> and  $\epsilon$ -FeSi alloys were laser heated up to  $\sim 1907 \text{ K}$  at  $\sim 49 \text{ GPa}$  and to  $\sim 2219 \text{ K}$  at  $\sim 54 \text{ GPa}$ , respectively. No phase transformation was observed in either sample, indicating that these silicon-rich Fe-Si alloys are relatively stable under high pressures and high temperatures.

## 4. Discussion

### 4.1. Isothermal Compression at 300 K

[13] Different results were reported in recent studies on the compressibility of  $\epsilon$ -FeSi [Ross, 1994; Knittle and Williams, 1995; Sarrao *et al.*, 1994; Wood *et al.*, 1995; Guyot *et al.*, 1997; Vocadlo *et al.*, 1999] (Table 6). Most of the studies show that  $\epsilon$ -FeSi has a bulk modulus between 160 and 180 GPa. Our experimental technique and pressure range are similar to that used by Knittle and Williams [1995], but a significantly higher bulk modulus and lower pressure derivative of the bulk modulus is observed in their study. As shown in Figure 5d, their compression data are systematically higher than that of this study, indicating that the lower, incorrect lattice parameter (see Table 6) of  $V_0 = 6.701(\pm 0.032) \text{ cm}^3/\text{mol}$  for  $\epsilon$ -FeSi under ambient conditions used by Knittle and Williams [1995] significantly affects their results. Analyzing the static compression data of Knittle and Williams [1995] using  $V_0 = 6.790(\pm 0.007) \text{ cm}^3/\text{mol}$  from this study,  $K_{0T}$  is found to be  $155.6(\pm 4.6) \text{ GPa}$  with  $K'_{0T} = 6.31(\pm 0.78)$ .

[14] A plot of the molar volume of the Fe-Si alloys versus pressure (Figure 6) reveals that the compression curves of hcp-Fe, hcp-Fe<sub>85</sub>Si<sub>15</sub>, and  $\epsilon$ -FeSi are almost identical to each other when extrapolated over 100 GPa, indicating that substitution of silicon into iron would lower the density of iron, but has little effect on the volume and compressibility of iron alloys at high pressures. This result is consistent with the conclusion of Zhang and Guyot [1999] that substitution of Si in iron would not significantly change the compressibility of the iron-rich Fe-Si alloy.

### 4.2. Thermal EOS Calculation

[15] To estimate the simultaneous effects of pressure and temperature on the EOS of iron-rich Fe-Si alloys, we have

**Table 2.** Static Compression Data for hcp-Fe<sub>85</sub>Si<sub>15</sub><sup>a</sup>

Run	$P$ , GPa	$\sigma$ ( $P$ ), GPa	$a$ , Å	$\sigma$ ( $a$ ), Å	$c$ , Å	$\sigma$ ( $c$ ), Å	$V/V_{01}$	$\sigma$ ( $V/V_{01}$ )	$c/a$
Fe79Si636 <sup>b</sup>	4.5	0.2	2.5040	0.0060	4.0890	0.0110	0.9571	0.0053	1.6330
Fe79Si635 <sup>b</sup>	6.7	0.5	2.4980	0.0050	4.0540	0.0070	0.9444	0.0041	1.6229
Fe79Si547 <sup>b</sup>	6.7	1.3	2.4923	0.0050	4.0502	0.0050	0.9392	0.0039	1.6251
Fe79Si634 <sup>b</sup>	9.6	1.1	2.4890	0.0060	4.0080	0.0080	0.9269	0.0048	1.6103
Fe79Si608	15.9 <sup>c</sup>	0.8	2.4475	0.0050	3.9600	0.0050	0.8855	0.0038	1.6180
Fe79Si609	17.2	0.9	2.4535	0.0050	3.9691	0.0050	0.8918	0.0038	1.6177
Fe79Si633 <sup>b</sup>	17.4	1.9	2.4570	0.0050	3.9720	0.0060	0.8951	0.0039	1.6166
Fe79Si545 <sup>b</sup>	21.0	1.1	2.4406	0.0057	3.9947	0.0088	0.8883	0.0046	1.6368
Fe79Si610	21.0	1.2	2.4410	0.0060	3.9710	0.0060	0.8833	0.0045	1.6268
Fe79Si611	22.8	1.0	2.4380	0.0050	3.9450	0.0070	0.8754	0.0039	1.6181
Fe79Si612	24.0	1.2	2.4320	0.0100	3.9690	0.0160	0.8763	0.0080	1.6320
Fe79Si518	24.3	1.1	2.4345	0.0072	3.9612	0.0100	0.8764	0.0056	1.6271
Fe79Si519	24.5	1.3	2.4316	0.0063	3.9599	0.0080	0.8741	0.0049	1.6285
Fe79Si544 <sup>b</sup>	24.7	1.2	2.4350	0.0059	3.9250	0.0068	0.8688	0.0045	1.6119
Fe79Si520	26.1	1.5	2.4262	0.0067	3.9447	0.0088	0.8668	0.0052	1.6259
Fe79Si613	26.5	1.2	2.4280	0.0060	3.9160	0.0070	0.8618	0.0045	1.6129
Fe79Si522	26.9	1.6	2.4260	0.0077	3.9292	0.0106	0.8633	0.0060	1.6196
Fe79Si521	27.0	1.5	2.4290	0.0078	3.9247	0.0108	0.8644	0.0060	1.6158
Fe79Si523	28.6	1.9	2.4208	0.0065	3.9236	0.0081	0.8584	0.0049	1.6208
Fe79Si614	29.1	1.4	2.4220	0.0060	3.9070	0.0070	0.8556	0.0045	1.6131
Fe79Si524	30.0	1.4	2.4201	0.0065	3.9182	0.0082	0.8567	0.0049	1.6190
Fe79Si632 <sup>b</sup>	30.0	1.4	2.4270	0.0060	3.9030	0.0070	0.8582	0.0045	1.6082
Fe79Si615	31.5	1.6	2.4150	0.0060	3.8970	0.0070	0.8485	0.0045	1.6137
Fe79Si525	31.7	1.8	2.4135	0.0065	3.9076	0.0082	0.8497	0.0049	1.6191
Fe79Si543 <sup>b</sup>	33.4	1.7	2.4197	0.0069	3.8899	0.0088	0.8502	0.0052	1.6076
Fe79Si526	33.8	1.9	2.4147	0.0069	3.9006	0.0089	0.8490	0.0052	1.6154
Fe79Si616	34.6	1.7	2.4090	0.0060	3.8890	0.0080	0.8425	0.0045	1.6144
Fe79Si527	34.8	1.7	2.4009	0.0080	3.9013	0.0085	0.8395	0.0059	1.6249
Fe79Si528	36.4	1.9	2.3989	0.0073	3.8965	0.0077	0.8371	0.0054	1.6243
Fe79Si617	37.0	1.8	2.4000	0.0060	3.8890	0.0070	0.8362	0.0044	1.6204
Fe79Si529	38.1	2.1	2.3952	0.0075	3.8898	0.0079	0.8331	0.0055	1.6240
Fe79Si618	39.1	2.0	2.3950	0.0060	3.8790	0.0070	0.8306	0.0044	1.6196
Fe79Si530	39.4	2.1	2.3891	0.0078	3.8893	0.0082	0.8287	0.0057	1.6279
Fe79Si542 <sup>b</sup>	39.9	2.0	2.3912	0.0072	3.8825	0.0075	0.8287	0.0052	1.6237
Fe79Si619	40.8	2.1	2.3930	0.0060	3.8730	0.0070	0.8279	0.0044	1.6185
Fe79Si531	41.0	2.1	2.3850	0.0081	3.8792	0.0086	0.8237	0.0059	1.6265
Fe79Si620	42.2	2.3	2.3880	0.0060	3.8670	0.0070	0.8232	0.0044	1.6193
Fe79Si631 <sup>b</sup>	44.4	2.5	2.3880	0.0060	3.8540	0.0070	0.8204	0.0044	1.6139
Fe79Si621	44.4	2.5	2.3840	0.0050	3.8440	0.0080	0.8156	0.0038	1.6124
Fe79Si622	45.9	2.6	2.3810	0.0060	3.8480	0.0070	0.8144	0.0044	1.6161
Fe79Si533	45.9	2.4	2.3733	0.0064	3.8745	0.0065	0.8147	0.0046	1.6325
Fe79Si534	46.3	2.5	2.3711	0.0052	3.8768	0.0052	0.8137	0.0037	1.6350
Fe79Si541 <sup>b</sup>	46.6	2.5	2.3742	0.0061	3.8466	0.0102	0.8094	0.0047	1.6202
Fe79Si623	48.1	2.7	2.3790	0.0050	3.8400	0.0060	0.8113	0.0036	1.6141
Fe79Si624	48.6	2.7	2.3780	0.0050	3.8370	0.0060	0.8100	0.0036	1.6135
Fe79Si535	49.1	2.8	2.3715	0.0067	3.8486	0.0086	0.8080	0.0049	1.6229
Fe79Si625	50.3	2.8	2.3740	0.0050	3.8330	0.0060	0.8064	0.0036	1.6146
Fe79Si536	50.5	2.8	2.3705	0.0060	3.8596	0.0073	0.8096	0.0044	1.6282
Fe79Si630 <sup>b</sup>	50.7	2.9	2.3740	0.0050	3.8330	0.0060	0.8064	0.0036	1.6146
Fe79Si626	51.4	2.9	2.3710	0.0050	3.8270	0.0060	0.8031	0.0036	1.6141
Fe79Si537	51.8	2.9	2.3701	0.0061	3.8268	0.0102	0.8025	0.0047	1.6146
Fe79Si539 <sup>b</sup>	52.9	3.1	2.3683	0.0065	3.8145	0.0080	0.7987	0.0047	1.6106
Fe79Si627	52.9	3.0	2.3690	0.0050	3.8190	0.0050	0.8001	0.0035	1.6121
Fe79Si538	53.3	3.1	2.3674	0.0063	3.8132	0.0076	0.7978	0.0045	1.6107
Fe79Si628	54.1	3.1	2.3680	0.0050	3.8130	0.0060	0.7982	0.0036	1.6102
Fe79Si629	54.3	3.1	2.3680	0.0050	3.8190	0.0060	0.7994	0.0036	1.6128

<sup>a</sup> $V_{02}/V_{01} = 0.9851 (\pm 0.0032)$ . Au was used as the pressure calibrant [Heinz and Jeanloz, 1984a].

<sup>b</sup>Collected during the process of decreasing pressure.

<sup>c</sup>This file (Fe79Si608 at 15.9 GPa) was not included in the BM EOS fit because the X-ray peaks of hcp-Fe<sub>85</sub>Si<sub>15</sub> were very weak.

calculated the thermal EOS of hcp-Fe and the hcp-Fe<sub>85</sub>Si<sub>15</sub> alloy using the Mie-Grüneisen EOS. Since bcc Fe-Si alloys have thermodynamic properties similar to those of iron under high pressures and high temperatures [Zhang and Guyot, 1999], it is reasonable to assume that hcp-Fe<sub>85</sub>Si<sub>15</sub> also has thermodynamic parameters similar to those of hcp-Fe. The parameters used in calculating the EOS of hcp-Fe and hcp-Fe<sub>85</sub>Si<sub>15</sub> in this study are listed in Table 7 [Mata-

ssov, 1977; Jeanloz, 1979; Jephcoat et al., 1986; Mao et al., 1990; Uchida et al., 2001]. The Grüneisen parameter ( $\gamma_0$ ) and  $\partial \ln \gamma / \partial \ln V$  ( $q$ ) of hcp-Fe measured by shock-wave experiments are used in this study [Jeanloz, 1979]. The reference isotherm of hcp-Fe [Jephcoat et al., 1986; Mao et al., 1990; Uchida et al., 2001] and hcp-Fe<sub>85</sub>Si<sub>15</sub> at 300 K is calculated using the BM EOS [Birch, 1978]. The thermal EOS of Fe and Fe<sub>85</sub>Si<sub>15</sub> is then calculated from the

**Table 3.** Static Compression Data for Fe<sub>71</sub>Si<sub>29</sub><sup>a</sup>

Run	$P$ , GPa	$\sigma$ ( $P$ ), GPa	$a$ , Å	$\sigma$ ( $a$ ), Å	$V/V_0$	$\sigma$ ( $V/V_0$ )
Fe17Si401	2.8	0.3	2.7994	0.0025	0.9879	0.0026
Fe17Si402	2.9	0.3	2.7992	0.0026	0.9877	0.0028
Fe17Si403	3.1	0.4	2.7979	0.0028	0.9863	0.0030
Fe17Si502	3.6	0.7	2.7916	0.0055	0.9796	0.0058
Fe17Si404	4.2	0.3	2.7934	0.0014	0.9815	0.0015
Fe17Si405	5.4	0.3	2.7876	0.0022	0.9754	0.0023
Fe17Si406	7.0	0.4	2.7819	0.0017	0.9695	0.0018
Fe17Si407	8.1	0.3	2.7771	0.0020	0.9645	0.0021
Fe17Si408	10.5	0.4	2.7691	0.0025	0.9562	0.0026
Fe17Si409	11.8	0.6	2.7602	0.0020	0.9470	0.0021
Fe17Si410	14.0	0.6	2.7508	0.0019	0.9373	0.0019
Fe17Si412	17.0	1.1	2.7408	0.0020	0.9271	0.0020
Fe17Si413	18.9	1.3	2.7387	0.0030	0.9250	0.0030
Fe17Si414	21.5	1.1	2.7330	0.0014	0.9192	0.0014
Fe17Si415	22.7	0.9	2.7270	0.0036	0.9132	0.0036
Fe17Si507	24.6	1.0	2.7306	0.0055	0.9168	0.0055
Fe17Si416	24.9	1.2	2.7214	0.0018	0.9076	0.0018
Fe17Si423 <sup>b</sup>	26.3	1.2	2.7233	0.0062	0.9095	0.0062
Fe17Si417	26.5	1.3	2.7176	0.0051	0.9038	0.0051
Fe17Si418	27.5	1.5	2.7140	0.0049	0.9002	0.0049
Fe17Si419	30.1	1.9	2.7058	0.0048	0.8921	0.0047
Fe17Si420	31.5	2.1	2.7023	0.0047	0.8886	0.0046
Fe17Si422 <sup>b</sup>	32.6	1.9	2.7035	0.0041	0.8898	0.0040
Fe17Si421	33.8	1.8	2.6966	0.0048	0.8830	0.0047
Fe17Si510	40.0	2.0	2.6884	0.0049	0.8750	0.0048
Fe17Si511	47.4	2.4	2.6739	0.0039	0.8609	0.0038
Fe17Si512	54.5	2.7	2.6613	0.0025	0.8488	0.0024

<sup>a</sup> $a_0 = 2.8108(\pm 0.0020)$  Å. Au was used as the pressure calibrant [Heinz and Jeanloz, 1984a].

<sup>b</sup>Collected during the process of decreasing pressure.

reference isotherm by use of the Mie-Grüneisen equation [McQueen et al., 1970]:

$$P_i(V) = P_{300}(V) + \frac{\gamma}{V} [E_i(T_i, \Theta) - E_{300}(300, \Theta)], \quad (1)$$

where  $P_{300}(V)$  is the pressure at the reference isotherm (300 K),  $\gamma$  is the Grüneisen parameter,  $V$  is the volume,  $\Theta$  is the Debye temperature, and  $E_i(T_i, \Theta)$  and  $E_{300}(300, \Theta)$  are the thermal energies at temperatures  $T_i$  and 300 K, respectively. The thermal energies are calculated using

$$E(T, \Theta) = \left( \frac{9nRT}{x^3} \int_0^x \frac{x^3}{e^x - 1} dx \right) + E_e \quad (2)$$

with

$$x = \frac{\Theta(V)}{T}, \quad (3)$$

$$\gamma = \gamma_0 \left( \frac{V}{V_0} \right)^q = - \frac{d \ln \Theta}{d \ln V}, \quad (4)$$

$$\Theta = \Theta_0 \exp \left\{ \frac{\gamma_0}{q} \left[ 1 - \left( \frac{V}{V_0} \right)^q \right] \right\}. \quad (5)$$

Here  $E_e$  is the electronic contribution of the energy [Boness and Brown, 1986; Anderson and Ahrens, 1994], and the Grüneisen parameter and the Debye temperature are considered to be only functions of volume [Matassov,

1977], i.e., the quasi-harmonic approximation was used. The electronic energy is

$$E_e = \int_0^T C_e dT, \quad (6)$$

where  $C_e$  is the electronic contribution to the heat capacity and  $T$  is the temperature.  $C_e$  data calculated by Boness and Brown [1986] are used both for Fe and Fe<sub>85</sub>Si<sub>15</sub>.

[16] The reference adiabatic EOS is generated by using the BM EOS with  $K_{0S} = K_{0T}(1 + \alpha\gamma T)$  and  $K'_{0S} \sim K'_{0T}$

**Table 4.** Static Compression Data for  $\epsilon$ -FeSi<sup>a</sup>

Run	$P$ , GPa	$\sigma$ ( $P$ ), GPa	$a$ , Å	$\sigma$ ( $a$ ), Å	$V/V_0$	$\sigma$ ( $V/V_0$ )
FeSi201	0.6	0.1	4.4840	0.0018	0.9996	0.0012
FeSi101	1.2	0.3	4.4768	0.0038	0.9948	0.0025
FeSi134 <sup>b</sup>	1.5	0.7	4.4834	0.0046	0.9992	0.0031
FeSi102	1.5	0.3	4.4743	0.0042	0.9931	0.0028
FeSi219 <sup>b</sup>	1.6	0.3	4.4781	0.0024	0.9957	0.0016
FeSi202	1.9	0.4	4.4695	0.0071	0.9899	0.0047
FeSi103	4.1	0.2	4.4524	0.0025	0.9786	0.0016
FeSi203	4.2	0.5	4.4464	0.0064	0.9747	0.0042
FeSi204	6.9	0.2	4.4267	0.0049	0.9618	0.0032
FeSi104	7.5	0.7	4.4312	0.0035	0.9647	0.0023
FeSi218 <sup>b</sup>	8.1	0.4	4.4387	0.0042	0.9696	0.0028
FeSi205	9.5	0.4	4.4077	0.0046	0.9494	0.0030
FeSi105	10.0	0.9	4.4168	0.0038	0.9553	0.0025
FeSi133 <sup>b</sup>	10.1	0.5	4.4243	0.0048	0.9602	0.0031
FeSi132 <sup>b</sup>	10.3	0.5	4.4232	0.0049	0.9595	0.0032
FeSi206	12.5	0.5	4.3881	0.0040	0.9368	0.0026
FeSi106	13.5	0.6	4.3971	0.0044	0.9426	0.0028
FeSi207	17.5	1.0	4.3678	0.0043	0.9239	0.0027
FeSi108	18.3	1.2	4.3690	0.0021	0.9246	0.0013
FeSi107	18.7	1.0	4.3694	0.0026	0.9249	0.0017
FeSi208	22.4	0.9	4.3472	0.0048	0.9109	0.0030
FeSi109	23.6	1.0	4.3400	0.0043	0.9064	0.0027
FeSi209	23.7	1.0	4.3368	0.0049	0.9044	0.0031
FeSi110	23.9	1.0	4.3316	0.0046	0.9011	0.0029
FeSi215 <sup>b</sup>	24.0	1.1	4.3465	0.0049	0.9104	0.0031
FeSi111	25.9	1.3	4.3175	0.0073	0.8923	0.0045
FeSi210	27.1	1.2	4.3238	0.0048	0.8962	0.0030
FeSi113	29.1	1.8	4.3105	0.0040	0.8880	0.0025
FeSi130 <sup>b</sup>	29.3	1.7	4.2948	0.0019	0.8783	0.0012
FeSi214 <sup>b</sup>	29.6	1.7	4.3108	0.0054	0.8882	0.0033
FeSi112	32.6	1.7	4.2889	0.0049	0.8747	0.0030
FeSi211	32.7	1.8	4.2917	0.0070	0.8764	0.0043
FeSi114	32.9	1.7	4.2890	0.0040	0.8748	0.0024
FeSi213 <sup>b</sup>	33.1	1.6	4.2927	0.0083	0.8770	0.0051
FeSi115	33.3	1.8	4.2932	0.0024	0.8773	0.0015
FeSi212	34.3	1.8	4.2894	0.0077	0.8750	0.0047
FeSi116	36.4	2.2	4.2698	0.0104	0.8631	0.0063
FeSi118	37.0	1.9	4.2859	0.0102	0.8729	0.0062
FeSi129 <sup>b</sup>	38.8	2.3	4.2608	0.0092	0.8576	0.0056
FeSi117	40.2	2.3	4.2586	0.0102	0.8563	0.0062
FeSi119	43.4	3.5	4.2559	0.0090	0.8547	0.0054
FeSi122	44.2	2.2	4.2525	0.0072	0.8526	0.0043
FeSi121	44.9	2.3	4.2492	0.0045	0.8506	0.0027
FeSi124	45.7	2.5	4.2410	0.0076	0.8457	0.0045
FeSi127 <sup>b</sup>	45.8	2.3	4.2454	0.0032	0.8484	0.0019
FeSi128 <sup>b</sup>	45.9	2.4	4.2472	0.0096	0.8494	0.0058
FeSi123	46.2	2.8	4.2420	0.0049	0.8463	0.0029
FeSi120	46.8	3.8	4.2517	0.0051	0.8522	0.0031
FeSi126 <sup>b</sup>	48.3	2.4	4.2387	0.0084	0.8444	0.0050
FeSi125	50.7	2.5	4.2279	0.0040	0.8379	0.0024

<sup>a</sup> $a_0 = 4.4846(\pm 0.0015)$  Å. Au was used as the pressure calibrant [Heinz and Jeanloz, 1984a].

<sup>b</sup>Collected during the process of decreasing pressure.

**Table 5.** EOS Parameters of bcc-Fe<sub>85</sub>Si<sub>15</sub>, hcp-Fe<sub>85</sub>Si<sub>15</sub>, Fe<sub>71</sub>Si<sub>29</sub>, and  $\epsilon$ -FeSi

Composition	$V_0$ , cm <sup>3</sup> /mol	Structure	$K_{0T}$	$K'_{0T}$	Highest Pressure, GPa
Fe <sub>85</sub> Si <sub>15</sub>	6.986 ( $\pm 0.007$ )	bcc	157.8 ( $\pm 4.0$ )	5.26 ( $\pm 0.88$ )	13.6
Fe <sub>85</sub> Si <sub>15</sub>	6.882 ( $\pm 0.031$ )	hcp	141 ( $\pm 10$ )	5.70 ( $\pm 0.60$ )	54.3
Fe <sub>71</sub> Si <sub>29</sub>	6.687 ( $\pm 0.014$ )	B2	199.0 ( $\pm 5.3$ )	5.66 ( $\pm 0.61$ )	54.5
$\epsilon$ -FeSi	6.790 ( $\pm 0.007$ )	B20	184.7 ( $\pm 3.9$ )	4.75 ( $\pm 0.37$ )	50.7

(Table 7). High-temperature adiabats are then calculated from the reference adiabat by use of the Mie-Grüneisen equation, and the temperature along each adiabat is

$$T = T_0 \exp \left\{ \frac{\gamma_0}{q} \left[ 1 - \left( \frac{V}{V_0} \right)^q \right] \right\}. \quad (7)$$

[17] The Hugoniot curve is also calculated by use of the Mie-Grüneisen equation as follows [McQueen *et al.*, 1970]:

$$P_H = P_S + \frac{\gamma}{V} (E_H - E_S) \quad (8)$$

with

$$E_H = E_0 + \frac{(P_H + P_0)(V_0 - V)}{2}, \quad (9)$$

$$E_S = E_0 - \int_{V_0}^V P_S dV, \quad (10)$$

where  $P_H$  is the Hugoniot pressure,  $P_S$  is the pressure along the adiabat passing through  $P = 0$  GPa and  $T = 300$  K,  $E_H$  is the energy along the Hugoniot,  $E_S$  is the energy along the adiabat passing through  $P = 0$  GPa and  $T = 300$  K and  $E_0$ ,  $P_0$ , and  $V_0$  are energy, pressure, and volume at the initial state, respectively. Thus the Hugoniot pressure is

$$P_H = \frac{P_S + \frac{\gamma}{V} \int_{V_0}^V P_S dV}{1 - \frac{\gamma}{2} \left( \frac{V_0}{V} - 1 \right)}. \quad (11)$$

The calculated Hugoniot curve from our data is consistent with shock-wave experiments on Fe<sub>87</sub>Si<sub>13</sub>

(6.9 wt.% Si) [Marsh, 1980] (Figure 7). The calculated adiabat passing through  $P = 0$  GPa and  $T = 3000$  K for hcp-Fe<sub>85</sub>Si<sub>15</sub> shows that Fe-rich Fe-Si alloys have a lower density than pure iron under core conditions (Figure 8). The effect of melting on the density was observed to be less than a few percent (within the experimental error of the shock-wave measurements) at pressures relevant to the core [Jeanloz, 1979]. Therefore our calculated EOS of solid hcp-Fe and hcp-Fe<sub>85</sub>Si<sub>15</sub> can be useful in discussing the density deficit of the liquid outer core.

[18] Upon comparison with the PREM density profile (Figure 8), the calculated EOS of Fe<sub>85</sub>Si<sub>15</sub> are consistent with an outer core containing Si as the light alloying element. An outer core containing about 8–10 wt.% Si (assuming negligible volume change upon melting) and an inner core containing about 4 wt.% Si in iron can satisfy the density deficits in the core (Figure 8). Assuming a maximum silicon content in the core of 7.3 wt.% based on geochemical mass balance [Allègre *et al.*, 1995], a small amount of other light element(s) in addition to silicon may be needed to satisfy the density deficit of the outer core. However, the exact amount of the light element in the core depends on the temperature profile of the core and the thermoelastic properties of the alloyed iron [Poirier, 1994; Hillgren *et al.*, 2000].

### 4.3. Bulk Sound Velocity Calculation

[19] The bulk sound velocity of the core appears to be 3% higher than that of pure liquid iron [Ahrens, 1982; Anderson and Ahrens, 1994]. The change of the bulk sound velocity across the liquid outer core to the solid inner core is less than 1% [Dziewonski and Anderson, 1981], suggesting that melting probably has small effect on the bulk sound velocity of iron under core conditions. High-pressure X-ray diffraction experiments on liquid Fe-Si alloy show that, in contrast to liquid Fe-S alloy [Sanloup *et al.*, 2000], the presence of silicon in iron has a negligible effect on the compressibility of iron [Sanloup *et al.*, 2001]. Therefore if silicon is the dominant light element in the core, Fe-Si alloys must have higher bulk sound velocity

**Table 6.** Comparison of the Elastic Parameters of  $\epsilon$ -FeSi

Reference	Pressure Range, GPa	$K_0$ , GPa	$K'_0$	$V_0$ , cm <sup>3</sup> /mol	Technique
This study	51	185 ( $\pm 4$ )	4.8 ( $\pm 0.4$ )	6.790 ( $\pm 0.007$ )	X-ray diffraction in DAC
Ross [1994]	7	176 ( $\pm 3$ )	4 (fixed)	n.a.	single-crystal X-ray diffraction
Knittle and Williams [1995]	50	209 ( $\pm 6$ )	3.5 ( $\pm 0.4$ )	6.701 ( $\pm 0.032$ )	X-ray diffraction in DAC
Sarrao <i>et al.</i> [1994]	room pressure	173 <sup>a</sup>	n.a.	n.a.	ultrasonic spectroscopy
Wood <i>et al.</i> [1995]	9	160 ( $\pm 1$ )	4 (fixed)	6.794 ( $\pm 0.01$ )	neutron diffraction
Guyot <i>et al.</i> [1997]	8	172 ( $\pm 3$ )	4 (fixed)	6.805 ( $\pm 0.005$ )	X-ray diffraction in multianvil apparatus
Vocadlo <i>et al.</i> [1999]	calculation	227	3.9	6.692	first-principle calculations

<sup>a</sup>The adiabatic bulk modulus.

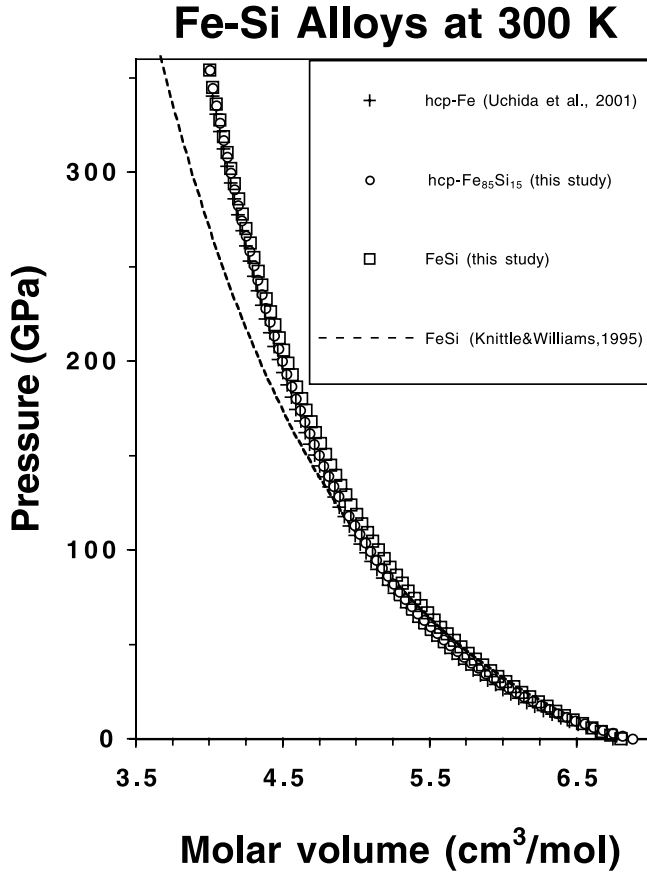


**Figure 6.** Comparison of molar volume (per unit molar atom) versus pressure at 300 K for hcp-Fe, hcp-Fe<sub>85</sub>Si<sub>15</sub>, and  $\epsilon$ -FeSi. Crosses, hcp-Fe [*Jephcoat et al.*, 1986; *Mao et al.*, 1990; *Uchida et al.*, 2001]; open circles, hcp-Fe<sub>85</sub>Si<sub>15</sub>; open squares,  $\epsilon$ -FeSi in B20 structure (extrapolated from this study); dashed line,  $\epsilon$ -FeSi extrapolated from the data given by *Knittle and Williams* [1995].

than that of iron under core conditions. The bulk sound velocity is defined as

$$V_{\phi} = \sqrt{\frac{K_S}{\rho}}, \quad (12)$$

where  $\rho$  is the density and  $K_S$  is the adiabatic bulk modulus. The adiabatic bulk modulus of iron-rich Fe-Si alloys at

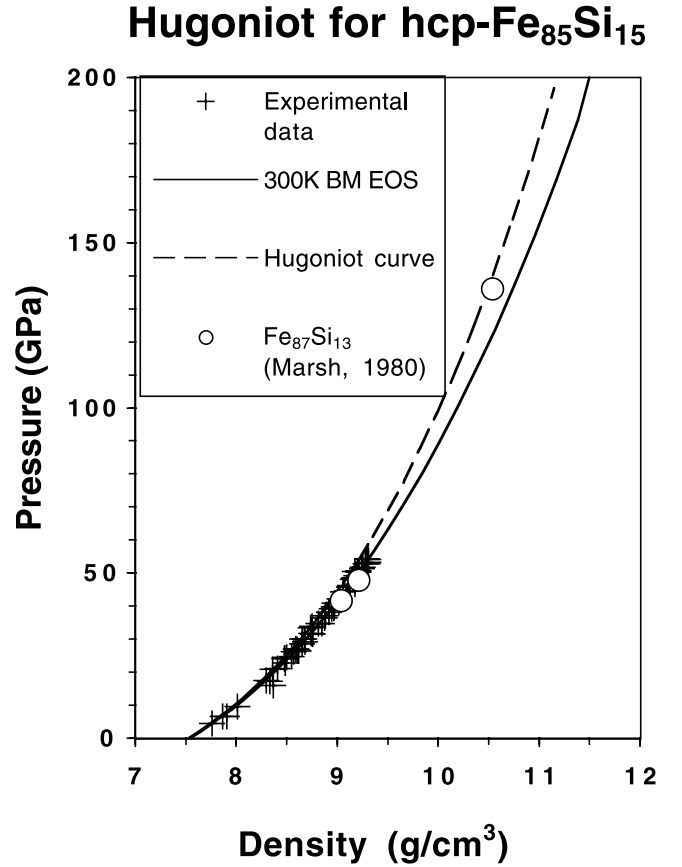


**Figure 7.** Hugoniot for hcp-Fe<sub>85</sub>Si<sub>15</sub> alloy. Solid line, 300 K BM EOS of the hcp-Fe<sub>85</sub>Si<sub>15</sub>; dashed line, calculated Hugoniot; open circles, shock-wave data for Fe<sub>87</sub>Si<sub>13</sub> [*Marsh*, 1980]; crosses, static compression data for hcp-Fe<sub>85</sub>Si<sub>15</sub> (this study).

ambient conditions can be calculated from ultrasonic measurements of the elasticity of these alloys [*Guinan and Beshers*, 1968; *Alberts and Wedepohl*, 1971; *Routbort et al.*, 1971; *Machova and Kadeckova*, 1977]. As shown in Figure 9, the adiabatic bulk modulus of the Fe-Si alloys in the bcc structure is independent of the silicon content and the shear modulus increases slightly with increasing the silicon concentration in the iron-rich Fe-Si alloys. As expected from the decrease in density of Fe-Si alloys, the bulk sound velocity, compressional wave velocity, and shear wave velocity of the iron-rich bcc Fe-Si alloys increase with

**Table 7.** Thermodynamic Properties of hcp-Fe and hcp-Fe<sub>85</sub>Si<sub>15</sub> at Ambient Conditions

Variable	hcp-Fe	Remark	hcp-Fe8wt.%Si	Remark
Molar volume ( $V_0$ )	6.84 ( $\pm 0.01$ ) cm <sup>3</sup>	<i>Uchida et al.</i> [2001]	6.88 ( $\pm 0.03$ ) cm <sup>3</sup>	this study
Isothermal bulk modulus ( $K_{0T}$ )	135 ( $\pm 19$ ) GPa	<i>Uchida et al.</i> [2001]	141 ( $\pm 10$ ) GPa	this study
Pressure derivative of $K_{0T}$ ( $K'_{0T}$ )	6.0 ( $\pm 0.4$ )	<i>Uchida et al.</i> [2001]	5.70 ( $\pm 0.6$ )	this study
Adiabatic bulk modulus ( $K_{0S}$ ) <sup>a</sup>	140 ( $\pm 20$ ) GPa	calculated	146 ( $\pm 10$ ) GPa	calculated
Heat capacity ( $C_v$ ) <sup>b</sup>	23.1 ( $\pm 6.2$ ) J/mol/K	calculated	24.3 ( $\pm 5.8$ ) J/mol/K	calculated
Thermal expansion ( $\alpha$ ) <sup>c</sup>	5.5 ( $\pm 0.4$ ) $\times 10^{-5}$ K <sup>-1</sup>	<i>Uchida et al.</i> [2001]	5.5 ( $\pm 0.4$ ) $\times 10^{-5}$ K <sup>-1</sup>	assumed
Debye temperature ( $\Theta$ )	464 K	<i>Matassov</i> [1977]	421 K	<i>Matassov</i> [1977]
Grüneisen parameter ( $\gamma_0$ ) <sup>c</sup>	2.2 ( $\pm 0.5$ )	<i>Jeanloz</i> [1979]	2.2 ( $\pm 0.5$ )	assumed
$\partial \ln \gamma / \partial \ln V$ ( $q$ ) <sup>c</sup>	1.62 ( $\pm 0.37$ )	<i>Jeanloz</i> [1979]	1.62 ( $\pm 0.37$ )	assumed

<sup>a</sup> $K_{0S}$  is calculated from  $K_{0S} = K_{0T} (1 + \alpha \gamma T)$ .

<sup>b</sup> $C_v$  is calculated from  $C_v = \alpha K_{0T} V / \gamma$ .

<sup>c</sup>Thermal expansion coefficient, Grüneisen parameter and  $\partial \ln \gamma / \partial \ln V$  of hcp-Fe<sub>85</sub>Si<sub>15</sub> are assumed to be the same as that of hcp-Fe.

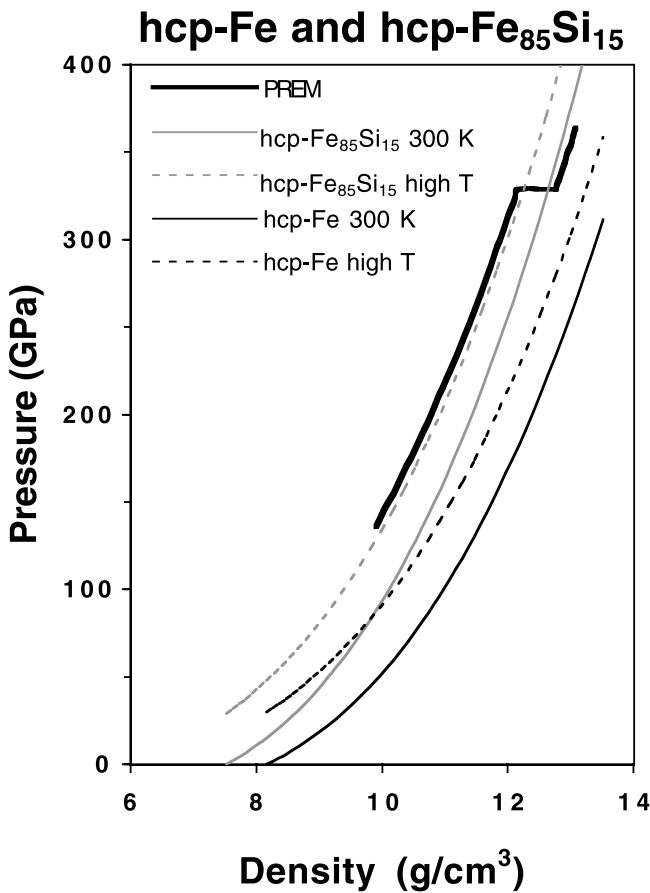


**Figure 8.** Calculated adiabats of hcp-Fe and hcp-Fe<sub>85</sub>Si<sub>15</sub> compared to the PREM model. The temperature for the adiabat of the hcp-Fe<sub>85</sub>Si<sub>15</sub> passing through  $P = 0$  GPa and  $T = 3000$  K at the core-mantle boundary is about 4948 K and is about 6300 K at inner core-outer core boundary. Thick black line, PREM; thin black line, an adiabat passing through  $P = 0$  GPa and  $T = 300$  K for hcp-Fe; dashed black line, an adiabat passing through  $P = 0$  GPa and  $T = 3000$  K for hcp-Fe; thin gray line, an adiabat passing through  $P = 0$  GPa and  $T = 300$  K for hcp-Fe<sub>85</sub>Si<sub>15</sub>; dashed gray line, an adiabat passing through  $P = 0$  GPa and  $T = 3000$  K for hcp-Fe<sub>85</sub>Si<sub>15</sub>.

increasing Si content (Figure 10). Addition of 8 wt.% Si increases the bulk sound velocity of bcc-Fe by approximately 3% (Figure 10). It was shown previously that substitution of silicon in hcp-Fe would lower the density, but would not significantly change the compressibility at high pressures; therefore addition of silicon into hcp-Fe would also increase the bulk sound velocity, consistent with silicon being a candidate light element in the core [Anderson and Ahrens, 1994].

[20] The calculated bulk sound velocity of hcp-Fe<sub>85</sub>Si<sub>15</sub> is higher than that of hcp-Fe under core conditions. However, the extrapolation of the bulk modulus to core conditions is compromised by the error on  $K'_0$  as well as the neglect of higher-order coefficients (terms beyond fourth order in strain) in the BM EOS. Precise experimental measurements on the elasticity and thermodynamic properties of Fe-Si alloys at higher pressure are needed in order to constrain the

bulk sound velocity of Fe-Si alloys under core conditions in a better way.

### 5. Conclusions

[21] Candidate light elements in the core are restricted by the following three constraints: lower density than pure iron, higher bulk sound velocity than iron, and freezing point depression of iron under core conditions [Poirier, 1994; Yang and Secco, 1999; Hillgren et al., 2000]. It has been demonstrated in this study that substitution of silicon in iron would lower the density, but would not significantly change the compressibility of iron at high pressures. Silicon, as the sole light alloying component in the core, can produce a sufficiently large reduction in the density. Addition of silicon into iron increases the bulk sound velocity of iron, consistent with silicon being a candidate light element in the core. Finally, it is expected from the phase diagram of Fe-Si system at ambient pressure [Kusbaschewski, 1982] that addition of silicon into iron lowers the melting point of iron under these conditions. The melting temperatures observed for Fe17wt.%Si up to 5.5 GPa are lower than those of pure iron [Yang and Secco, 1999].

[22] Despite the previous exclusion of Si as the primary alloying element in the outer core based on the relatively high  $K_0$  and low  $K'_0$  of  $\epsilon$ -FeSi [Knittle and Williams, 1995; Williams and Knittle, 1997], our results based on the elasticity of three Fe-Si alloys (Fe<sub>85</sub>Si<sub>15</sub>, Fe<sub>71</sub>Si<sub>29</sub>, and  $\epsilon$ -FeSi) indicate that silicon could be a significant light element

### Elastic moduli of Fe-Si alloys at 300 K

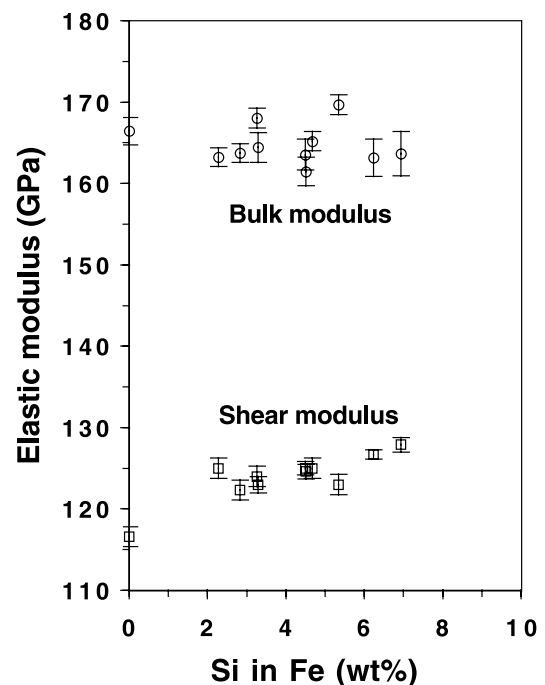


**Figure 9.** Adiabatic bulk moduli (open circles) and shear moduli (open squares) calculated from ultrasonic measurements of the elasticity of the iron-rich Fe-Si alloys at ambient conditions [Guinan and Beshers, 1968; Alberts and Wedepohl, 1971; Routbort et al., 1971; Machova and Kadeckova, 1977]. All alloys were in bcc structure.

## $V_\phi$ , $V_p$ , $V_s$ of Fe-Si alloys at 300 K

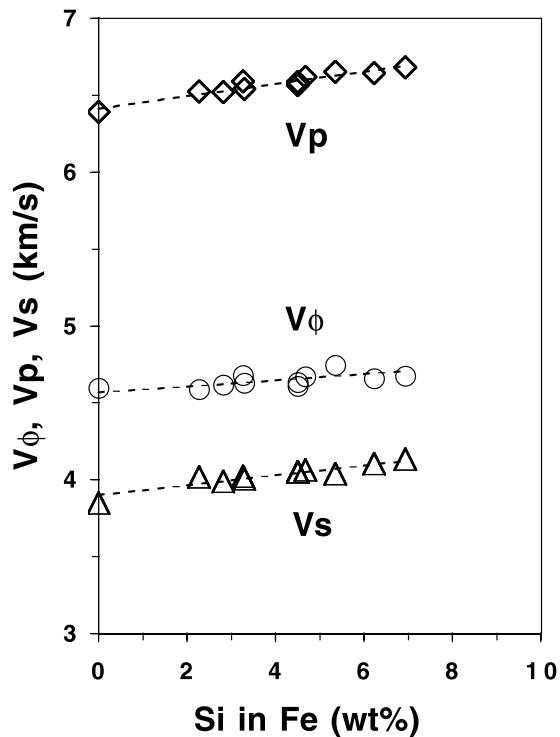


**Figure 10.** Bulk sound velocities (open circles), compressional wave velocities (open diamonds), and shear wave velocities (open triangles) of iron-rich Fe-Si alloys calculated from ultrasonic measurements at ambient conditions [Guinan and Beshers, 1968; Alberts and Wedepohl, 1971; Roubort et al., 1971; Machova and Kadeckova, 1977].

in the core. However, the possible presence of other light elements cannot be excluded on the basis of these results.

[23] **Acknowledgments.** We thank GSECARS at APS, ANL for providing the synchrotron beam and the William M. Keck Foundation for funding the facility. We also thank William Bassett, Eugene Huang, James Devine, and Wendy Mao for their assistance with the experiments and the manuscript and Ian Steele for his help with the electron microprobe analyses. This research is supported by NSF grant EAR-9974373 to D.L.H.

## References

Ahrens, T. J., Constraints on core composition from shock-wave data, *Philos. Trans. R. Soc. London, Ser. A*, 306, 37–47, 1982.

Alberts, H. L., and P. T. Wedepohl, Elastic constants of dilute iron-silicon alloy single crystals below room temperature, *Physica*, 53, 571–580, 1971.

Allègre, C. J., J. P. Poirier, E. Humblert, and A. W. Hofmann, The chemical composition of the Earth, *Earth Planet. Sci. Lett.*, 134, 515–526, 1995.

Anderson, W. W., and T. J. Ahrens, An equation of state for liquid iron and implications for the Earth's core, *J. Geophys. Res.*, 99, 4273–4284, 1994.

Balchan, A. S., and G. R. Cowan, Shock compression of two iron-silicon alloys to 2.7 megabars, *J. Geophys. Res.*, 71, 3577–3588, 1966.

Bassett, W. A., A. H. Shen, M. Bucknum, and I. M. Chou, Hydrothermal studies in a new diamond anvil cell up to 10 GPa and from  $-190^\circ\text{C}$  to  $1200^\circ\text{C}$ , *Pure Appl. Geophys.*, 141, 487–495, 1993.

Birch, F., Elasticity and constitution of the Earth's interior, *J. Geophys. Res.*, 57, 227–286, 1952.

Birch, F., Finite strain isotherm and velocities for single-crystal and polycrystalline NaCl at high pressures and 300 K, *J. Geophys. Res.*, 83, 1257–1268, 1978.

Boness, D. A., and J. M. Brown, The electronic thermodynamics of iron under Earth core conditions, *Phys. Earth Planet. Inter.*, 42, 227–240, 1986.

Dziewonski, A. M., and D. L. Anderson, Preliminary reference Earth model, *Phys. Earth Planet. Inter.*, 25, 297–356, 1981.

Fiquet, G., J. Badro, F. Guyot, H. Requardt, and M. Krisch, Sound velocities in iron to 110 gigapascals, *Science*, 291, 468–471, 2001.

Gessmann, C. K., B. J. Wood, D. C. Rubie, and M. R. Kilburn, Solubility of silicon in liquid metal at high pressure: Implications for the composition of the Earth's core, *Earth Planet. Sci. Lett.*, 184, 367–376, 2001.

Guinan, M. W., and D. N. Beshers, Pressure derivatives of the elastic constants of  $\alpha$ -iron to 10 kbs, *J. Phys. Chem. Solids*, 29, 541–549, 1968.

Guyot, F., J. Zhang, I. Martinez, J. Matas, Y. Ricard, and M. Javoy,  $P$ - $V$ - $T$  measurements of iron silicide ( $\epsilon$ -FeSi): Implications for silicate-metal interactions in the early Earth, *Eur. J. Mineral.*, 9, 277–285, 1997.

Heinz, D. L., and R. Jeanloz, The equation of state of the gold calibration standard, *J. Appl. Phys.*, 55, 885–893, 1984a.

Heinz, D. L., and R. Jeanloz, Compression of the B2 high-pressure phase of NaCl, *Phys. Rev. B*, 30, 6045–6050, 1984b.

Hillgren, V. J., C. K. Gessmann, and J. Li, An experimental perspective on the light element in Earth's core, in *Origin of the Earth and the Moon*, edited by R. M. Canup and K. Righter, pp. 245–263, Univ. of Ariz. Press, Tucson, 2000.

Huang, E., W. A. Bassett, and P. Tao, Study of bcc-hcp iron phase transition by synchrotron radiation, in *High-Pressure Research in Mineral Physics*, edited by M. H. Manghni and Y. Syono, pp. 165–172, TERRAPUB, Tokyo, 1987.

Jeanloz, R., Properties of iron at high pressures and the state of the core, *J. Geophys. Res.*, 84, 6059–6069, 1979.

Jeanloz, R., Finite-strain equation of state for high-pressure phases, *Geophys. Res. Lett.*, 8, 1219–1222, 1981.

Jephcoat, A., and P. Olson, In the inner core of the Earth pure iron?, *Nature*, 325, 332–335, 1987.

Jephcoat, A., H. K. Mao, and P. M. Bell, Static compression of iron to 78 GPa with rare gas solids as pressure-transmitting media, *J. Geophys. Res.*, 91, 4677–4684, 1986.

Khalaff, K., and K. Schubert, Kristallstruktur von  $\text{Fe}_2\text{Si}(h)$ , *J. Less Common Met.*, 35, 341–345, 1974.

Knittle, E., and R. Jeanloz, Simulating the core-mantle boundary: An experimental study of high-pressure reactions between silicates and liquid iron, *Geophys. Res. Lett.*, 16, 609–612, 1989.

Knittle, E., and R. Jeanloz, Earth's core-mantle boundary: Results of experiments at high pressures and temperatures, *Science*, 251, 1438–1443, 1991.

Knittle, E., and Q. Williams, Static compression of  $\epsilon$ -FeSi and evaluation of reduced silicon as a deep earth constituent, *Geophys. Res. Lett.*, 22, 445–448, 1995.

Kusbaschewski, O., *Iron-Binary Phase Diagram*, Springer-Verlag, New York, 1982.

Lin, J. F., D. L. Heinz, A. J. Campbell, J. M. Devine, and G. Shen, Iron-silicon alloy in the Earth's core?, *Science*, 295, 313–315, 2002.

Machova, A., and S. Kadeckova, Elastic constants of iron-silicon alloy single crystals, *Czech. J. Phys. B*, 27, 555–563, 1977.

Mao, H. K., Y. Wu, L. C. Chen, and J. F. Shu, Static compression of iron to 300 GPa and  $\text{Fe}_{0.8}\text{Ni}_{0.2}$  alloy to 260 GPa: Implications for composition of the core, *J. Geophys. Res.*, 95, 21,737–21,742, 1990.

Mao, H. K., et al., Phonon density of states of iron up to 153 GPa, *Science*, 292, 914–916, 2001.

Marsh, S. P., *LASL Shock Hugoniot Data*, Univ. of Calif. Press, Berkeley, 1980.

Matassov, G., The electrical conductivity of iron-silicon alloys at high pressures and the Earth's core, Ph.D. thesis, *Lawrence Livermore Laboratory Rep. UCRL-52322*, 1977.

McQueen, R. G., S. P. Marsh, J. P. Taylor, J. N. Fritz, and W. J. Carter, *High-Velocity Impact Phenomena*, edited by R. Kinslow, pp. 293–417, Academic, San Diego, Calif., 1970.

Pauling, L., and A. M. Soldate, The nature of the bonds in the iron silicide FeSi and related crystals, *Acta Crystallogr.*, 1, 212–216, 1948.

Piermarini, G. J., S. Block, and J. D. Barnett, Hydrostatic limits in liquids and solids to 100 kbar, *J. Appl. Phys.*, 44, 5377–5382, 1973.

Piermarini, G. J., S. Block, J. D. Barnett, and R. A. Forman, Calibration of the pressure dependence of the  $R_1$  ruby fluorescence line to 195 kbar, *J. Appl. Phys.*, 46, 2774–2780, 1975.

Poirier, J. P., Light elements in the Earth's core: A critical review, *Phys. Earth Planet. Inter.*, 85, 319–337, 1994.

Ringwood, A. E., Chemical evolution of the terrestrial planets, *Geochim. Cosmochim. Acta*, 30, 41–104, 1966.

Ross, N. L., High-pressure single-crystal X-ray diffraction study of  $\epsilon$ -FeSi, *Acta Crystallogr., Sect. A*, 52, C-530, 1994.

- Routbort, J. L., C. N. Reid, E. S. Fisher, and D. J. Dever, High-temperature elastic constants and the phase stability of silicon-iron, *Acta Met.*, *19*, 1307–1316, 1971.
- Sanloup, C., F. Guyot, P. Gillet, G. Fiquet, M. Mezouar, and I. Martinez, Density measurements of liquid Fe-S alloys at high-pressure, *Geophys. Res. Lett.*, *27*, 811–814, 2000.
- Sanloup, C., et al., Physical properties of liquid Fe alloys at high pressure and their bearings on the nature of metallic planetary cores: Implications for the Earth, Mars and the Gailean satellites, *Lunar Planet. Sci. XXXII*, abstract 1877, 2001.
- Sarrao, J. L., D. Mandrus, A. Migliori, Z. Fisk, and E. Bucher, Elastic properties of FeSi, *Physica B*, *199–200*, 478–479, 1994.
- Stixrude, L., E. Wasserman, and R. E. Cohen, Composition and temperature of Earth's inner core, *J. Geophys. Res.*, *102*, 24,729–24,739, 1997.
- Uchida, T., Y. Wang, M. L. Rivers, and S. R. Sutton, Stability field and thermal equation of state of  $\epsilon$ -iron determined by synchrotron X-ray diffraction in a multianvil apparatus, *J. Geophys. Res.*, *106*, 21,799–21,810, 2001.
- Vocadlo, L., G. D. Price, and I. G. Wood, Crystal structure, compressibility and possible phase transitions in  $\epsilon$ -FeSi studied by first-principles pseudopotential calculations, *Acta Crystallogr. Sect. B*, *55*, 484–493, 1999.
- Williams, Q., and E. Knittle, Constraints on core chemistry from the pressure dependence of the bulk modulus, *Phys. Earth Planet. Inter.*, *100*, 49–59, 1997.
- Wood, I. G., T. D. Chaplin, W. I. F. David, S. Hull, G. D. Price, and J. N. Street, Compressibility of FeSi between 0 and 9 GPa, determined by high-pressure time-of-flight neutron powder diffraction, *J. Phys. Condens. Matter*, *7*, L475–L479, 1995.
- Yang, H., and R. A. Secco, Melting boundary of Fe-17%Si up to 5.5 GPa and the timing of core formation, *Geophys. Res. Lett.*, *26*, 263–266, 1999.
- Zhang, J., and F. Guyot, Thermal equation of state of iron and Fe<sub>0.91</sub>Si<sub>0.09</sub>, *Phys. Chem. Miner.*, *26*, 206–211, 1999.
- 
- A. J. Campbell, D. L. Heinz, and J.-F. Lin, Department of the Geophysical Sciences, University of Chicago, Chicago, IL 60637, USA. (j.lin@gl.ciw.edu)
- G. Shen, Consortium for Advanced Radiation Sources, University of Chicago, Chicago, IL 60637, USA.